Tracking in Wireless Sensor Networks Using Particle Filtering: Physical Layer Considerations

Onur Ozdemir, *Student Member, IEEE*, Ruixin Niu, *Member, IEEE*, and Pramod K. Varshney, *Fellow, IEEE*

***Abstract*—In this paper, a new framework for target tracking in a wireless sensor network using particle filters is proposed. Under this framework, the imperfect nature of the wireless communication channels between sensors and the fusion center along with some physical layer design parameters of the network are incorporated in the tracking algorithm based on particle filters. We call this approach "channel-aware particle filtering." Channel-aware particle filtering schemes are derived for different wireless channel models and receiver architectures. Furthermore, we derive the posterior Cramér–Rao lower bounds (PCRLBs) for our proposed channel-aware particle filters. Simulation results are presented to demonstrate that the tracking performance of the channel-aware particle filters can reach their theoretical performance bounds even with relatively small number of sensors and they have superior performance compared to channel-unaware particle filters.**

***Index Terms*—Channel-aware signal processing, particle filters, posterior Cramér–Rao lower bound, wireless communication channels, wireless sensor networks (WSNs).**

I. Introduction

A WIRELESS sensor network (WSN) employs low-cost densely deployed sensors that have very limited resources, such as energy and communication bandwidth. They also have limited sensing and communication ranges. Therefore, the issues that are related to these limitations need to be investigated before using WSNs in a specific application.

In this paper, we focus on target tracking using low-cost and low-power wireless sensors that are densely deployed in an area of interest. These sensors process their raw observations, quantize them, and send their quantized measurements to a central processing node, which is called the fusion center, through noisy and fading wireless channels. The fusion center then processes these received measurements to perform the tracking task. A generic system framework is illustrated in Fig. 1.

In this framework, there are unavoidable constraints that should not be neglected and need to be analyzed. First of all, wireless communication channels between sensors and the fusion center are not ideal. Second, sensors have inherent limitations imposed by the current technology in terms of sensing range, computational capability and energy. Although some work has been done in the past to solve target localization and tracking problems with wireless sensors [1]–[8], to the best of our knowledge, existing tracking algorithms do not address both of these limitations at the same time. In [1]–[3], the signals received by the fusion center are modeled as analog measurements corrupted by white Gaussian noise (WGN). This scheme is not practical for many wireless sensor networks since communication within the network has to be kept limited to conserve available resources, such as energy and bandwidth. In [4]–[6], particle filtering algorithms for target tracking using quantized data in WSNs have been proposed, however wireless channel imperfections have not been considered as part of the tracking problem. In [7] and [8], target localization methods have been developed based on quantized sensor data again assuming perfect communication channels between sensors and the fusion center. In our recent work [9], we introduced a channel-aware approach for the problem of target localization using WSNs. The issue of communication constraints in the context of distributed detection has been investigated in [10]–[16]. However, except for our previous work in [17], communication constraints in the context of tracking have not been analyzed explicitly in the literature. In a target tracking scenario where a large number of wireless sensors are deployed in a particular area, we can not always guarantee a line-of-sight between sensors and the fusion center. Therefore, wireless communication is carried out via long-range communication schemes rather than bluetooth or infrared, resulting in lower fidelity. Furthermore, in order to use the available resources efficiently, each sensor has to transmit a low-power signal at a low data rate to communicate with the fusion center. This motivates the development of efficient tracking algorithms incorporating the imperfect nature of communication channels as well as based on the constraints of limited resources in a WSN. In fact, we show in this paper that, for a given power requirement and a given number of sensors, channel-aware data processing at the

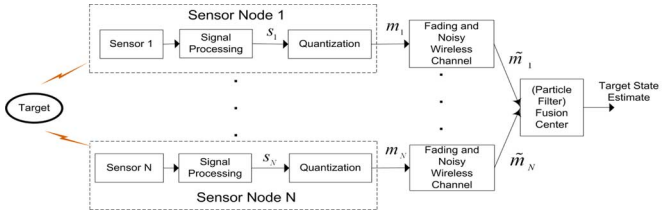

Fig. 1. Generic system model. s_i is the raw sensor measurement of the ith sensor, m_i is the quantized sensor measurement, and $\tilde{m}_i$ is the channel-corrupted sensor measurement received by the fusion center from the ith sensor, where $i = 1, \ldots, N$.

Manuscript received April 11, 2008; accepted December 18, 2008. First published February 06, 2009; current version published April 15, 2009. The associate editor coordinating the review of this manuscript and approving it for publication was Dr. Aleksandar Dogandzic. This work was supported in part by U.S. Army Research Office under Award W911 NF-06-1-0250. This work was presented in part at the Fortieth Asilomar Conference on Signals, Systems and Computers, Pacific Grove, CA, October 2006.

The authors are with Syracuse University, Department of Electrical Engineering and Computer Science, Syracuse, NY 13244 USA (e-mail: oozdemir@syr.edu; rniu@ecs.syr.edu; varshney@ecs.syr.edu).

Color versions of one or more of the figures in this paper are available online at http://ieeexplore.ieee.org.

Digital Object Identifier 10.1109/TSP.2009.2014818

fusion center can significantly mitigate the degradation in the tracking performance resulting from non-ideal communication channels without adding any communication overhead to the system.

Tracking a moving target using a WSN [1]–[5] is a typical nonlinear sequential estimation problem. With the recent advances in computation power, application of Monte Carlo based statistical signal processing, i.e., particle filtering, for sequential estimation of unknown states of a nonlinear dynamical system has become quite popular and practical. Based on the fact that sequential Monte Carlo methods enable us to incorporate any statistical information we have about the specific system directly in the tracking algorithm, we propose a new target tracking approach based on sequential Monte Carlo signal processing, more specifically particle filtering, incorporating the constraints related to WSNs. To be more specific, as an extension to our previous work in [17], where each channel link between sensors and the fusion center was modeled as a binary symmetric channel (BSC), here we create a more general framework where we develop different tracking approaches using particle filters and compute their corresponding posterior Cramér–Rao lower bounds (PCRLBs) incorporating various physical layer parameters, namely realistic wireless fading channel statistics as well as different reception and decoding strategies. Note that although our tracking approach is more general than the one that deals only with channel imperfections, we refer to our approach as "channel-aware" since it incorporates channel statistics whereas the classical approach which assumes perfect channels will be referred to as "channel-unaware" throughout this paper.

The organization of this paper is as follows. We formulate the problem of target tracking using quantized data in a WSN in Section II. In Section III, we give a brief introduction to Bayesian sequential estimation and provide the motivation behind using particle filtering for our tracking problem. We introduce our channel-aware approach and derive three different channel-aware particle filtering algorithms in Section IV. The first tracking algorithm is developed for a hard-decoding link design. It incorporates the bit error probabilities of the channel which is modeled as a binary channel (BC) (note that although BSC is a very general model, it is only a special case of BC). The second and the third tracking algorithms are specifically developed for soft-decoding link designs assuming Rayleigh fading channels with phase coherent and phase noncoherent reception, respectively. In Section V, we present the methodology for PCRLB computation and derive the PCRLBs for our channel-aware particle filters. In Section VI, simulation results are presented to assess the performance of our developed particle filtering algorithms. We also evaluate the impact of physical layer on tracking performance by comparing the performance of our algorithms with each other under identical conditions. Finally, concluding remarks are presented in Section VII.

II. Problem Formulation

As mentioned in the previous section, the problem we seek to solve is tracking a moving target in a wireless sensor network environment where densely deployed homogeneous and low-cost wireless sensors are employed, and the channels are nonideal. All the sensors report to a fusion center which sequentially estimates the target state, i.e., the position and the velocity of the target, based on received local sensor data. We assume that the sensors are stationary and the fusion center has perfect information about the locations of sensors. Note that the deployment scheme of sensors is not an issue since our approach is capable of handling any kind of deployment, e.g., random, in a grid or in some other deterministic manner, conditioned on the fact that location information for each sensor is available at the fusion center.

A. Target Dynamic Model

We consider a single target moving in a two-dimensional Cartesian coordinate plane. Target dynamics is defined by the 4-dimensional state vector

$$\tilde{\mathbf{x}}_k = [\xi_{tk} \quad \eta_{tk} \quad \dot{\xi}_{tk} \quad \dot{\eta}_{tk}]^T \tag{1}$$

where ξ_{tk} and η_{tk} denote the coordinates of the target in the horizontal and the vertical directions with the corresponding velocities $\dot{\xi}_{tk}$ and $\dot{\eta}_{tk}$, respectively, at time k. The superscript T denotes the transpose operation. Target motion is defined by the following white noise acceleration model [18]:

$$\tilde{\mathbf{x}}_k = \tilde{\mathbf{F}}\,\tilde{\mathbf{x}}_{k-1} + \tilde{\boldsymbol{\upsilon}}_k \tag{2}$$

where

$$\tilde{\mathbf{F}} = \begin{bmatrix} 1 & 0 & T & 0 \\ 0 & 1 & 0 & T \\ 0 & 0 & 1 & 0 \\ 0 & 0 & 0 & 1 \end{bmatrix} \tag{3}$$

and $\tilde{\boldsymbol{\upsilon}}_k$ is the process noise which is assumed to be white, zero-mean and Gaussian with the following covariance matrix

$$\tilde{\mathbf{Q}} = q \begin{bmatrix} \frac{T^3}{3} & 0 & \frac{T^2}{2} & 0 \\ 0 & \frac{T^3}{3} & 0 & \frac{T^2}{2} \\ \frac{T^2}{2} & 0 & T & 0 \\ 0 & \frac{T^2}{2} & 0 & T \end{bmatrix} \tag{4}$$

where T and q denote the time interval between adjacent sensor measurements and the process noise parameter, respectively. It is assumed that the fusion center has perfect information about the target state-space model (2) as well as the process noise statistics.

B. Measurement Model

The target is assumed to be any source that follows the power attenuation model provided below. At any given time k, the signal power received at the ith sensor is the following:

$$P_{ik} = \frac{P_k d_0^n}{(d_{ik})^n} \tag{5}$$

where P_k denotes the target signal power at a reference distance of d_0 from the target at time k, n is the signal decay exponent, and d_{ik} is the distance between the target and the ith sensor:

$$d_{ik} = \sqrt{(\xi_i - \xi_{tk})^2 + (\eta_i - \eta_{tk})^2}. \tag{6}$$

In (6), (ξ_i, η_i) and (ξ_{tk}, η_{tk}) are the coordinates of the ith sensor and the target at time k, respectively. The received signal at each sensor is given by

$$s_{ik} = a_{ik} + w_{ik} \tag{7}$$

where $a_{ik} = \sqrt{P_{ik}}$ is the true measurement, and w_{ik} is the noise term modeled as zero mean additive white Gaussian noise (AWGN), i.e., $w_{ik} \sim \mathcal{N}(0, \sigma_w^2)$, which represents the cumulative effects of sensor background noise and the modeling error of signal parameters. Although P_k is stationary, it is often not constant and subject to small variations. Therefore, the dynamics of P_k can be modeled as

$$P_k = P_{k-1} + \beta_k \tag{8}$$

where β_k is the zero mean AWGN, i.e., $\beta_k \sim \mathcal{N}(0, \sigma_\beta^2)$. Since P_k is modeled as a dynamic process, the original state vector $\tilde{\mathbf{x}}_k$ given in (1) can be augmented with P_k to form the augmented state vector

$$\mathbf{x}_k = [P_k \quad \tilde{\mathbf{x}}_k^T]^T. \tag{9}$$

Then the augmented state dynamic model can be expressed as $\mathbf{x}_k = \mathbf{F}\,\mathbf{x}_{k-1} + \boldsymbol{v}_k$, where $\boldsymbol{v}_k \sim \mathcal{N}(\mathbf{0}, \mathbf{Q})$ and

$$\mathbf{F} = \begin{bmatrix} 1 & \mathbf{0} \\ \mathbf{0} & \tilde{\mathbf{F}} \end{bmatrix}, \quad \mathbf{Q} = \begin{bmatrix} \sigma_\beta^2 & \mathbf{0} \\ \mathbf{0} & \tilde{\mathbf{Q}} \end{bmatrix}. \tag{10}$$

The general assumptions we make about our measurement model are as follows. Without loss of generality, the reference distance d_0 and the signal decay exponent n are assumed to be unity and 2, respectively. The fusion center is assumed to have all the information about the noise statistics. Note that the signal decay exponent n and the sensor noise statistics can be empirically determined off-line for the system under consideration. We also assume that sensor noises w_{ik} as well as the wireless links between the sensors and the fusion center are independent across sensors. Although it is not required for our approach to work, the sensors are assumed to have identical noise variances for simplicity.

It was previously mentioned in Section I that the received signal s_{ik} at each sensor is locally quantized before being sent to the fusion center. The main reason for quantization is to decrease the amount of communication so that the energy consumption is reduced. The quantized observation model at sensor i is given by

$$m_{ik} = \begin{cases} 0, & \gamma_{i0} < s_{ik} < \gamma_{i1} \\ 1, & \gamma_{i1} < s_{ik} < \gamma_{i2} \\ \vdots & \vdots \\ L-1, & \gamma_{i(L-1)} < s_{ik} < \gamma_{iL} \end{cases} \tag{11}$$

where m_{ik} is the quantized measurement of the ith sensor and $\gamma_{i0}, \ldots, \gamma_{iL}$ are the predetermined thresholds for a $K = \log_2 L$ bit quantizer. Note that $\gamma_{i0} = -\infty$ and $\gamma_{iL} = \infty$. Based on (11), the transmitted observations from sensors to the fusion center can be denoted in vector form as $\mathbf{M}_k = [m_{1k} \quad m_{2k} \quad \ldots \quad m_{Nk}]^T$, where N is the total number of sensors deployed in the area of interest. If one neglects the effects of unreliable wireless channels between sensors and the fusion center, then the fusion center could be assumed to receive an exact replica of $\mathbf{M}_k$ in order to perform the assigned task, which is target tracking in this paper. However, this assumption is not always valid for a WSN because of the reasons explained in Section I, i.e., the channels between wireless sensors and the fusion center are unreliable. Let $\mathbf{Y}_k$ denote the observation vector at the fusion center after transmission through the imperfect channels

$$\mathbf{Y}_k = [\tilde{m}_{1k} \quad \tilde{m}_{2k} \quad \ldots \quad \tilde{m}_{Nk}]^T \tag{12}$$

where $\tilde{m}_{ik}$'s are the quantized sensor measurements corrupted by the imperfect wireless channels. Multiplicative fading due to multipath effects and additive channel noise are the main factors that cause corruption which will be discussed in more detail in Section IV. Based on the information contained in $\mathbf{Y}_k$, the fusion center needs to sequentially estimate the target state $\mathbf{x}_k$. Note that the measurement model is highly nonlinear due to quantization at the local sensors and corruptions from the wireless channels.

III. Nonlinear Non-Gaussian Bayesian Sequential Estimation Using Particle Filtering

Bayesian sequential estimation, also known as Bayesian filtering, is the most commonly used framework for tracking applications. In Bayesian filtering, the tracking algorithm recursively calculates the belief in the state $\mathbf{x}_k$ based on the observations $\mathbf{Y}$ from time 1 to time k, namely the posterior distribution (or the filtering distribution) $p(\mathbf{x}_k \,|\, \mathbf{Y}_{1:k})$, where $\mathbf{Y}_{1:k} = \{\mathbf{Y}_i, i = 1, \ldots, k\}$. In order to recursively calculate the posterior distribution, we need to have three distributions [21], namely the initial state distribution $p(\mathbf{x}_0)$ at time 0, the state transition model $p(\mathbf{x}_k|\mathbf{x}_{k-1})$ which represents the state dynamics and the likelihood function $p(\mathbf{Y}_k|\mathbf{x}_k)$ which depends on the observation model.

It is known that Kalman filter provides an optimal solution to the Bayesian sequential problem for linear/Gaussian systems. In the case of nonlinear/Gaussian systems, extended Kalman filter (EKF) can be used to provide a suboptimal solution by linearizing the nonlinear state dynamics and/or measurement equations locally. However, it has been shown [5] that, even for linear/Gaussian systems, when the sensor measurements are quantized, EKF fails to provide an acceptable performance especially when the number of quantization levels is small. For our tracking problem, in addition to the nonlinear mapping from the target state to the sensor observations (7), the final measurement model at the fusion center consists of both quantized and channel-corrupted sensor observations (12) resulting in a highly nonlinear and non-Gaussian system. Therefore, we propose to employ a particle filter to solve our Bayesian sequential estimation problem. It is known that particle filtering provides an approximate solution to the classical Bayesian sequential estimation problem by approximating the posterior distribution $p(\mathbf{x}_k|\mathbf{Y}_{1:k})$ using a set of weighted samples, also called particles, $\{\mathbf{x}_k^{(j)}, w_k^{(j)}\}_{j=1}^M$, where $w_k^{(j)}$ denotes the weight of the particle $\mathbf{x}_k^{(j)}$ at time k and M is the total number of particles [21]. In this paper, we employ sequential importance resampling (SIR) particle filtering algorithm [21] to solve our nonlinear Bayesian sequential estimation problem. Although the SIR particle filter can be inefficient and sensitive to outliers [21] depending on the specific problem, we will show in Section VI that its performance is quite satisfactory for our tracking problem, or in other words its performance is very close to its theoretical bound,

namely the PCRLB. The advantage of the SIR particle filter is that it is very easy to implement and computationally more efficient compared to other variants of particle filters. Here, we do not discuss the details of the algorithm for the sake of brevity and refer the interested reader to [21] and [22]. The initial set of particles is drawn from a prior distribution $\pi(\mathbf{x}_0)$ which is assumed to represent $p(\mathbf{x}_0)$. The state-space distribution $p(\mathbf{x}_k|\mathbf{x}_{k-1})$ that is needed for the prediction stage is derived by using (2). Therefore, the only remaining distribution that has to be calculated for the sequential estimation problem is the observation likelihood function $p(\mathbf{Y}_k|\mathbf{x}_k^{(j)})$ which depends on both the sensor measurement model and the characteristics of physical layer of the WSN including the statistical properties of the wireless channels between sensors and the fusion center. The calculation of $p(\mathbf{Y}_k|\mathbf{x}_k^{(j)})$ is investigated under various physical-layer architectures in Section IV.

IV. Particle Filtering With Physical-Layer Considerations

The system designer has to make a choice about how to design the physical (link) layer, i.e., the communication architecture, of a WSN and different design choices result in different performances for a specific application. The functions of the physical layer that need to be designed include modulation schemes, data encryption techniques, transceiver architectures and decoding schemes at the receiver. In this paper, we consider only two physical layer functions, where a design choice is made. The first one is the decoding scheme at the fusion center and there are only two choices. The link layer can be designed such that the fusion center either makes a hard decision for each bit (or data symbol) before performing the tracking task or uses received measurements directly to track the target. The former and the latter link layer designs are called hard-decoding link and soft-decoding link, respectively. For a hard-decoding link, if the communication channel statistics and the parameters of the network physical layer are known, the probability of making a wrong decision can be calculated and the corresponding channel can be modeled as a binary-channel (BC). However, for a soft-decoding link, both the knowledge of the channel statistics and the physical layer parameters need to be incorporated directly in the tracking algorithm since no hard decision is made beforehand. In this paper, we analyze the system assuming BCs for hard-decoding links and Rayleigh flat fading channels for soft-decoding links as in [13], between sensors and the fusion center. As for the second link layer function to be designed, we consider the receiver architecture at the fusion center. We assume two reception techniques which are phase coherent and phase noncoherent reception. Note that the former reception technique requires phase information of the received signal whereas the latter does not. As a summary, we develop three different target tracking algorithms based on particle filters and derive their performance bounds (PCRLBs) for three different physical-layer designs, namely, the BC (hard-decoding link with either coherent or noncoherent reception), Rayleigh fading channel (soft-decoding link) with coherent reception, and Rayleigh fading channel (soft-decoding link) with noncoherent reception.

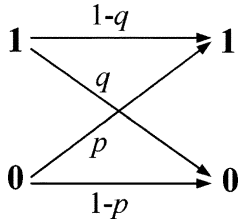

Fig. 2. Binary channel.

Throughout this section, we omit the time index k in our derivations unless otherwise required. For a given time step, we can use the sensor observation model in (7) with the Gaussian noise assumption and the quantization model in (11), to derive $p(m_i|\mathbf{x})$, the probability of a quantized sensor measurement taking a specific value conditioned on the target state:

$$p(m_i|\mathbf{x}) = \begin{cases} Q\left(\frac{\gamma_{i0}-a_i}{\sigma_w}\right) - Q\left(\frac{\gamma_{i1}-a_i}{\sigma_w}\right), & m_i = 0 \\ Q\left(\frac{\gamma_{i1}-a_i}{\sigma_w}\right) - Q\left(\frac{\gamma_{i2}-a_i}{\sigma_w}\right), & m_i = 1 \\ \vdots & \vdots \\ Q\left(\frac{\gamma_{i(L-1)}-a_i}{\sigma_w}\right) - Q\left(\frac{\gamma_{iL}-a_i}{\sigma_w}\right), & m_i = L-1 \end{cases} \tag{13}$$

where $Q(\cdot)$ is the complementary distribution function of the standard Gaussian distribution defined as

$$Q(x) = \int_x^\infty \frac{1}{\sqrt{2\pi}} e^{-\frac{t^2}{2}}\, dt. \tag{14}$$

Note that a_i in (13) implicitly includes (5) and (6), so it should be noted that the sensor observation model $p(m_i|\mathbf{x})$ is a function of the target's signal power and the target's position, i.e., the first three elements of the augmented target state vector $\mathbf{x}$ in (9).

A. Hard-Decoding Binary Channel

Fig. 2 depicts a general binary channel model with bit error probabilities p and q. Note that the received observation statistics at the fusion center is dependent on the channel statistics, i.e., on p and q. Here, we assume, for simplicity, that each channel between the sensors and the fusion center has identical bit error probabilities and channel links are independent of each other. However, note that our methodology will still work for more general BC models, i.e., even if different channels have different bit error probabilities.

Using the channel model in Fig. 2, the probability of a received sensor observation $\tilde{m}_i$ taking a specific value m, given the target state, can be written as

$$p(\tilde{m}_i = m|\mathbf{x}) = \sum_{m_i=0}^{L-1} p(\tilde{m}_i = m|m_i) p(m_i|\mathbf{x}). \tag{15}$$

Note that (15) uses the fact that $\mathbf{x}, m_i$ and $\tilde{m}_i$ form a Markov chain, i.e., $p(\tilde{m}_i|m_i, \mathbf{x}) = p(\tilde{m}_i|m_i)$. Channel statistics is represented by the first term in the summation, i.e., $p(\tilde{m}_i = m|m_i)$, in (15). For example, given a target state $\mathbf{x}$, if $L = 2$ is used to send the measurements through a BC, the probability of a received observation from sensor i being equal to 1 is $p(\tilde{m}_i = 1|\mathbf{x}) = p(m_i = 1|\mathbf{x})(1-q) + p(m_i = 0|\mathbf{x})p$. Since sensor

noises and wireless links are assumed to be independent, the likelihood function at the fusion center can be written as

$$p(\mathbf{Y}|\mathbf{x}) = \prod_{i=1}^{N} p(\tilde{m}_i|\mathbf{x}) = \prod_{i=1}^{N} \left[\sum_{m_i=0}^{L-1} p(\tilde{m}_i|m_i)\, p(m_i|\mathbf{x}) \right]. \quad (16)$$

Recall from Section III that the likelihood function derived in (16) was the only remaining distribution required for the SIR particle filtering algorithm to work. At a given time step k, it is straightforward from (16) to calculate the likelihood function for each particle $\mathbf{x}_k^{(j)}$

$$p\left(\mathbf{Y}_k|\mathbf{x}_k^{(j)}\right) = \prod_{i=1}^{N} \left[\sum_{m_i=0}^{L-1} p(\tilde{m}_i|m_i) p\left(m_i|\mathbf{x}_k^{(j)}\right) \right], \quad j = 1, \ldots, M. \quad (17)$$

Using (17), the particle filtering algorithm can now be applied to track the target.

B. Soft-Decoding in Rayleigh Fading Channel With Coherent Reception

Let $h_i e^{j\phi_i}$ denote the complex gain of the discrete-time Rayleigh fading channel between the ith sensor and the fusion center. It is assumed that the channel gain $h_i e^{j\phi_i}$ is stationary and ergodic, and it remains constant during a symbol transmission time. Note that h_i and ϕ_i are the fading envelope and the phase of the channel, respectively. Here, we simplify the analysis by assuming binary signaling ($L = 2$) and replace $\{0, 1\}$ by $\{-1, 1\}$ in (11), so that the effect of the fading channel reduces to a real scalar multiplication for phase coherent reception [13]. This is illustrated by using the received signal model for sensor i:

$$\tilde{r}_i = h_i e^{j\phi_i} m_i + v_i \quad (18)$$

where v_i is a zero-mean complex Gaussian noise with independent real and imaginary parts having identical variance σ_v^2, i.e., $v_i \sim \mathcal{CN}(0, 2\sigma_v^2)$. The notation $\mathcal{CN}$ represents complex Gaussian distribution. Without loss of generality, we assume that the channels have unit power, i.e., $h_i e^{j\phi_i} \sim \mathcal{CN}(0, 1)$, therefore $E[h_i^2] = 1$. The received measurement $\tilde{m}_i$ with the knowledge of the channel phase at the receiver can be expressed as

$$\tilde{m}_i = \mathrm{Re}\left\{\tilde{r}_i e^{-j\phi_i}\right\} = h_i m_i + \mathrm{Re}\left\{v_i e^{-j\phi_i}\right\}. \quad (19)$$

Note that the noise term in (19) is real WGN with variance σ_v^2, i.e., $\mathrm{Re}\{v_i e^{-j\phi_i}\} \sim \mathcal{N}(0, \sigma_v^2)$, based on the fact that v_i follows a circularly symmetric complex Gaussian distribution. With the unit power Rayleigh fading channel assumption, the probability density function (pdf) of h_i is given as

$$p(h_i) = 2h_i e^{-h_i^2}, \quad h_i \geq 0. \quad (20)$$

Then, it is straightforward to obtain the conditional pdf $p(\tilde{m}_i|m_i)$, i.e., the pdf of the transmitted signal $\tilde{m}_i$ given sensor observation m_i:

$$p(\tilde{m}_i|m_i) = \int_0^\infty p(\tilde{m}_i|h_i, m_i) p(h_i) dh_i. \quad (21)$$

Following the above assumptions and the same procedure, the conditional pdf $p(\tilde{m}_i|m_i)$ has been derived in [13] and given as follows:

$$p(\tilde{m}_i|m_i) = \frac{2\sigma_v}{\sqrt{2\pi}\,(1 + 2\sigma_v^2)} e^{\frac{-\tilde{m}_i^2}{2\sigma_v^2}} \times \left[1 + m_i \sqrt{2\pi} \alpha \tilde{m}_i e^{\frac{(\alpha \tilde{m}_i)^2}{2}} Q(-\alpha m_i \tilde{m}_i) \right] \quad (22)$$

where $\alpha = 1/(\sigma_v \sqrt{1 + 2\sigma_v^2})$. Then, it is easy to obtain

$$p(\tilde{m}_i|\mathbf{x}) = \sum_{m_i \in \{-1,1\}} p(\tilde{m}_i|m_i) p(m_i|\mathbf{x}) \quad (23)$$

where the terms in the summation are given in (22) and (13), respectively.

Following the same procedure as in the previous subsection with the assumption of independence between wireless links (Section II-B), the likelihood function for each particle, $\mathbf{x}_k^{(j)}$, to be used in the SIR particle filtering algorithm can be derived as follows:

$$p\left(\mathbf{Y}_k|\mathbf{x}_k^{(j)}\right) = \prod_{i=1}^{N} \left[\sum_{m_i \in \{-1,1\}} p(\tilde{m}_i|m_i) p\left(m_i|\mathbf{x}_k^{(j)}\right) \right], \quad j = 1, \ldots, M. \quad (24)$$

C. Soft-Decoding in Rayleigh Fading Channel With Noncoherent Reception

In this subsection, we analyze our final link layer design scenario where we employ the same wireless channel conditions and binary signaling as in Section IV-B. The only difference between the scenario in this subsection and that in the previous one is the particular reception scheme employed at the fusion center. Here, we assume that energy detection (ED) strategy is adopted at the fusion center, which is a phase noncoherent reception scheme and makes it possible to use sensor censoring [12], i.e., ON/OFF signaling at the sensors, where they remain silent for $m_i = 0$. Note that sensor censoring enables WSN to save energy thereby increase the network lifetime. Let r_i denote the received signal from sensor i before ED at the fusion center.

$$r_i = \begin{cases} v_i, & m_i = 0 \\ h_i e^{j\phi_i} + v_i, & m_i = 1 \end{cases} \quad (25)$$

where $v_i \sim \mathcal{CN}(0, 2\sigma_v^2)$, and $h_i e^{j\phi_i} \sim \mathcal{CN}(0, 1)$ (unit power Rayleigh fading channel). After ED, the observation model at the fusion center for the ith sensor is given as $\tilde{m}_i = |r_i|^2$.

Note that the notation $|\cdot|$ indicates the magnitude of a complex number. Then, it is straightforward to obtain the conditional pdf

$$p(\tilde{m}_i|m_i=0)=\frac{1}{2\sigma_v^2}e^{-\frac{\tilde{m}_i}{2\sigma_v^2}}$$
$$p(\tilde{m}_i|m_i=1)=\frac{1}{1+2\sigma_v^2}e^{-\frac{\tilde{m}_i}{1+2\sigma_v^2}}. \quad (26)$$

Similar to the previous section, the conditional pdf $p(\tilde{m}_i|\mathbf{x})$ can be written as

$$p(\tilde{m}_i|\mathbf{x})=\sum_{m_i=0}^{1}p(\tilde{m}_i|m_i)p(m_i|\mathbf{x}). \quad (27)$$

The same analysis as in the previous two subsections can be applied here to find the likelihood function for each particle,

$$p\left(\mathbf{Y}_k|\mathbf{x}_k^{(j)}\right)=\prod_{i=1}^{N}\left[\sum_{m_i=0}^{1}p(\tilde{m}_i|m_i)p\left(m_i|\mathbf{x}_k^{(j)}\right)\right],\quad j=1,\ldots,M. \quad (28)$$

V. Posterior Cramér–Rao Lower Bounds

In this section, we derive the tracking performance bounds, namely the Posterior Cramér–Rao lower bounds (PCRLBs), for the three different physical-layer models discussed in Section IV.

Let $\hat{\mathbf{x}}_k(\mathbf{Y}_{1:k})$ be an estimator of the state vector $\mathbf{x}_k$ at time k, given all the available measurements $\mathbf{Y}_{1:k}$ up to time k. Then, the mean square error (MSE) matrix of the estimation error at time k, B_k, is bounded below by the posterior Cramér–Rao lower bound (PCRLB) J_k^{-1} [22]

$$B_k=E\left\{[\hat{\mathbf{x}}_k(\mathbf{Y}_{1:k})-\mathbf{x}_k][\hat{\mathbf{x}}_k(\mathbf{Y}_{1:k})-\mathbf{x}_k]^T\right\}\geq J_k^{-1} \quad (29)$$

where J_k is the Fisher information matrix (FIM). In [23], Tichavský *et al.* provide a recursive approach to calculate the sequential FIM J_k:

$$J_{k+1}=D_k^{22}-D_k^{21}\left(J_k+D_k^{11}\right)^{-1}D_k^{12} \quad (30)$$

where

$$D_k^{11}=E\left\{-\Delta_{\mathbf{x}_k}^{\mathbf{x}_k}log\,p(\mathbf{x}_{k+1}|\mathbf{x}_k)\right\} \quad (31)$$
$$D_k^{12}=E\left\{-\Delta_{\mathbf{x}_k}^{\mathbf{x}_{k+1}}\log p(\mathbf{x}_{k+1}|\mathbf{x}_k)\right\} \quad (32)$$
$$D_k^{21}=E\left\{-\Delta_{\mathbf{x}_{k+1}}^{\mathbf{x}_k}\log p(\mathbf{x}_{k+1}|\mathbf{x}_k)\right\}=\left(D_k^{12}\right)^T \quad (33)$$
$$D_k^{22}=E\left\{-\Delta_{\mathbf{x}_{k+1}}^{\mathbf{x}_{k+1}}\log p(\mathbf{x}_{k+1}|\mathbf{x}_k)\right\}+E\left\{-\Delta_{\mathbf{x}_{k+1}}^{\mathbf{x}_{k+1}}\log p(\mathbf{Y}_{k+1}|\mathbf{x}_{k+1})\right\}=D_k^{22,a}+D_k^{22,b}. \quad (34)$$

The operator Δ in (31)–(34) is defined as $\Delta_{\Psi}^{\Theta}=\nabla_{\Psi}\nabla_{\Theta}^T$, where ∇ is the gradient operator expressed as

$$\nabla_{\mathbf{x}}=\left[\frac{\partial}{\partial x_1},\ldots,\frac{\partial}{\partial x_r}\right]^T. \quad (35)$$

Note that r in (35) denotes the dimension of $\mathbf{x}$. It is important to note that all the above expectations (31)–(34) are taken with respect to the joint probability distribution $p(\mathbf{x}_{0:k+1},\mathbf{Y}_{1:k+1})$. The initial FIM J_0 can be calculated from the *a priori* pdf $p(\mathbf{x}_0)$

$$J_0=E\left\{-\Delta_{\mathbf{x}_0}^{\mathbf{x}_0}\log\,p(\mathbf{x}_0)\right\}. \quad (36)$$

For our linear target dynamic model (2) and nonlinear measurement model explained in Section II-B, the recursion (31)–(34) become

$$D_k^{11}=\mathbf{F}^T\mathbf{Q}^{-1}\mathbf{F} \quad (37)$$
$$D_k^{12}=\left(D_k^{21}\right)^T=-\mathbf{F}^T\mathbf{Q}^{-1} \quad (38)$$
$$D_k^{22}=\mathbf{Q}^{-1}+D_k^{22,b}. \quad (39)$$

Note that the calculation of $D_k^{22,b}$ requires the exact knowledge of the observation likelihood function $p(\mathbf{Y}_{k+1}|\mathbf{x}_{k+1})$ and for most of the real world scenarios including our problem in this paper, $D_k^{22,b}$ does not have a closed-form solution. However, similar to the nonlinear filtering problem, Monte Carlo techniques can again be applied here to solve this problem [22].

Based on the fact that $\mathbf{x}_k,\mathbf{x}_{k+1}$ and $\mathbf{Y}_{k+1}$ form a Markov chain, the joint pdf for the expectation can be rewritten as follows:

$$p(\mathbf{x}_{0:k+1},\mathbf{Y}_{1:k+1})=p(\mathbf{x}_{0:k},\mathbf{Y}_{1:k})\cdot p(\mathbf{x}_{k+1}|\mathbf{x}_k).p(\mathbf{Y}_{k+1}|\mathbf{x}_{k+1}). \quad (40)$$

Using this property along with the target dynamic and measurement models described in Section II, it is straightforward to derive $D_k^{22,b}$ as

$$D_k^{22,b}=E_{p(\mathbf{x}_k)}\{\mathbf{\Lambda}^k\} \quad (41)$$

where $\mathbf{\Lambda}^k\in\mathbb{R}^5\times\mathbb{R}^5$ and its elements are defined as

$$\Lambda^k=-E_{p(\mathbf{x}_{k+1}|\mathbf{x}_k)p(\mathbf{Y}_{k+1}|\mathbf{x}_{k+1})}\left\{\Delta_{\mathbf{x}_{k+1}}^{\mathbf{x}_{k+1}}\times\log p(\mathbf{Y}_{k+1}|\mathbf{x}_{k+1})\right\}. \quad (42)$$

The outer integrations in (42) can be approximately evaluated by converting them into summations using Monte Carlo integration methodology. In order to do this, we first generate a set of samples $\mathbf{x}_{k+1}^{(j)}\sim p(\mathbf{x}_{k+1}|\mathbf{x}_{k,\text{true}})$ with identical weights $w_{k+1}^{(j)}=M^{-1}$, where $j=1,\ldots,M$. Then, the above expectations can be approximated as follows:

$$\Lambda^k\approx-\frac{1}{M}\sum_{j=1}^{M}E_{p\left(\mathbf{Y}_{k+1}|\mathbf{x}_{k+1}^{(j)}\right)}\left\{\Delta_{\mathbf{x}_{k+1}}^{\mathbf{x}_{k+1}}\log p(\mathbf{Y}_{k+1}|\mathbf{x}_{k+1})\right\}. \quad (43)$$

The final expectations with respect to $p(\mathbf{x}_k)$ in (41) can be obtained by averaging the above approximations (in (43)) over a number of Monte Carlo trials, i.e., over a number of sample tracks.

The PCRLBs for our tracking problem under three different physical layer models are obtained and stated in the following theorems.

Theorem 1: Given a hard-decoding binary channel, the PCRLB of a Bayesian sequential estimator, $\hat{\mathbf{x}}_k(\mathbf{Y}_{1:k})$, is given by

$$B_k = E\{[\hat{\mathbf{x}}_k(\mathbf{Y}_{1:k}) - \mathbf{x}_k][\hat{\mathbf{x}}_k(\mathbf{Y}_{1:k}) - \mathbf{x}_k]^T\} \geq J_k^{-1}$$

in which J_k is the recursive FIM. The recursion of J_k follows (30)–(39), where $\mathbf{\Lambda}^k$ is as follows:

$$\Lambda^k \approx \frac{1}{M}\sum_{j=1}^{M}\sum_{i=1}^{N}\sum_{\tilde{m}_{ik}=0}^{L-1}\frac{\nabla_{\mathbf{x}_k^{(j)}} p\left(\tilde{m}_{ik}|\mathbf{x}_k^{(j)}\right)\nabla_{\mathbf{x}_k^{(j)}}^T p\left(\tilde{m}_{ik}|\mathbf{x}_k^{(j)}\right)}{p\left(\tilde{m}_{ik}|\mathbf{x}_k^{(j)}\right)} \tag{44}$$

where the term $p(\tilde{m}_{ik}|\mathbf{x}_k^{(j)})$ is given in (15). Omitting the time index k for clarity, the expressions for the other terms in (44) are

$$\nabla_{\mathbf{x}} p(\tilde{m}_i|\mathbf{x}) = \sum_{m_i=0}^{L-1} p(\tilde{m}_i|m_i)\nabla_{\mathbf{x}} p(m_i|\mathbf{x}) \tag{45}$$

in which

$$\begin{aligned}
\frac{\partial p(m_i = l|\mathbf{x})}{\partial P} &= \frac{d_i^{-\frac{n}{2}}\lambda_{il}}{2\sqrt{2\pi}\sigma_w\sqrt{P}} \\
\frac{\partial p(m_i = l|\mathbf{x})}{\partial \xi_t} &= \frac{n a_i d_i^{-2}(\xi_i - \xi_t)\lambda_{il}}{2\sqrt{2\pi}\sigma_w} \\
\frac{\partial p(m_i = l|\mathbf{x})}{\partial \eta_t} &= \frac{n a_i d_i^{-2}(\eta_i - \eta_t)\lambda_{il}}{2\sqrt{2\pi}\sigma_w} \\
\frac{\partial p(m_i = l|\mathbf{x})}{\partial \dot{\xi}_t} &= \frac{\partial p(m_i = l|\mathbf{x})}{\partial \dot{\eta}_t} = 0
\end{aligned} \tag{46}$$

and

$$\lambda_{il} = \left[e^{-\frac{(\gamma_{il}-a_i)^2}{2\sigma_w^2}} - e^{-\frac{(\gamma_{i(l+1)}-a_i)^2}{2\sigma_w^2}}\right]. \tag{47}$$

Proof: See Appendix A. ∎

The PCRLBs for target location coordinates ξ_{tk} and η_{tk} are the $(1,1)$ and the $(2,2)$ elements of the inverse FIM J_k, respectively, i.e.,

$$\mathrm{MSE}(\hat{\xi}_{tk}) \geq \left[J_k^{-1}\right]_{11},\ \mathrm{MSE}(\hat{\eta}_{tk}) \geq \left[J_k^{-1}\right]_{22}. \tag{48}$$

Theorem 2: Given a soft-decoding Rayleigh fading channel with coherent reception, the PCRLB of a Bayesian sequential estimator, $\hat{\mathbf{x}}_k(\mathbf{Y}_{1:k})$, is given by $B_k = E\{[\hat{\mathbf{x}}_k(\mathbf{Y}_{1:k}) - \mathbf{x}_k][\hat{\mathbf{x}}_k(\mathbf{Y}_{1:k}) - \mathbf{x}_k]^T\} \geq J_k^{-1}$, in which J_k is the recursive FIM. The recursion of J_k follows (30)–(39), where $\mathbf{\Lambda}^k$ is given by (49), shown at the bottom of the page. The expressions for partial derivative terms, omitting the time index k, in (49) are

$$\nabla_{\mathbf{x}} p(\tilde{m}_i|\mathbf{x}) = \sum_{m_i\in\{-1,1\}} p(\tilde{m}_i|m_i)\nabla_{\mathbf{x}} p(m_i|\mathbf{x}) \tag{50}$$

where the conditional pdf $p(\tilde{m}_i|m_i)$ and the partial derivative terms are given in (22) and (46), respectively.

Proof: See Appendix B. ∎

We should mention that closed forms for the integrals in (49) do not exist. Therefore, numerical integration methods are needed for evaluating these integrals.

Theorem 3: Given a soft-decoding Rayleigh fading channel with noncoherent reception, the PCRLB of a Bayesian sequential estimator, $\hat{\mathbf{x}}_k(\mathbf{Y}_{1:k})$, is given by $B_k = E\{[\hat{\mathbf{x}}_k(\mathbf{Y}_{1:k}) - \mathbf{x}_k][\hat{\mathbf{x}}_k(\mathbf{Y}_{1:k}) - \mathbf{x}_k]^T\} \geq J_k^{-1}$, in which J_k is the recursive FIM. The recursion of J_k follows (30)–(39), where $\mathbf{\Lambda}^k$ is given as (51), shown at the bottom of the page. The expressions for partial derivative terms in (51) are

$$\nabla_{\mathbf{x}} p(\tilde{m}_i|\mathbf{x}) = \sum_{m_i=0}^{1} p(\tilde{m}_i|m_i)\nabla_{\mathbf{x}} p(m_i|\mathbf{x}) \tag{52}$$

where the conditional pdf $p(\tilde{m}_i|m_i)$ and the partial derivative terms are given in (26) and (46), respectively.

Proof: See Appendix C. ∎

Similar to the coherent reception case, closed forms for the integrals in (51) do not exist. Therefore, numerical integration methods are needed for evaluating these integrals.

VI. Simulation Results

In this section, we evaluate the tracking performance of our channel-aware particle filtering approach developed in Sections III–IV, for three different link layer designs. Sensors are assumed to be grid deployed in a 200 m × 200 m area. The number of sensors per unit area is adopted as the metric for sensor density and it is denoted by ρ. For simplicity, each sensor is assumed to employ identical thresholds for quantization, hence the sensor index i is omitted in γ_{il}. We also assume that sensor background noise has unit power, i.e., $\sigma_w^2 = 1$. For the target dynamic model, the following scenario is selected where all units are in meters, seconds and meters per second corresponding to distance, time and velocity measurements, respectively. The initial state distribution of the target $p(x_0)$ is assumed to be Gaussian with

$$\Lambda^k \approx \frac{1}{M}\sum_{j=1}^{M}\sum_{i=1}^{N}\int_{-\infty}^{\infty}\frac{\nabla_{\mathbf{x}_k^{(j)}} p\left(\tilde{m}_{ik}|\mathbf{x}_k^{(j)}\right)\nabla_{\mathbf{x}_k^{(j)}}^T p\left(\tilde{m}_{ik}|\mathbf{x}_k^{(j)}\right)}{p\left(\tilde{m}_{ik}|\mathbf{x}_k^{(j)}\right)} d\tilde{m}_{ik}. \tag{49}$$

$$\Lambda^k \approx \frac{1}{M}\sum_{j=1}^{M}\sum_{i=1}^{N}\int_{0}^{\infty}\frac{\nabla_{\mathbf{x}_k^{(j)}} p\left(\tilde{m}_{ik}|\mathbf{x}_k^{(j)}\right)\nabla_{\mathbf{x}_k^{(j)}}^T p\left(\tilde{m}_{ik}|\mathbf{x}_k^{(j)}\right)}{p\left(\tilde{m}_{ik}|\mathbf{x}_k^{(j)}\right)} d\tilde{m}_{ik}. \tag{51}$$

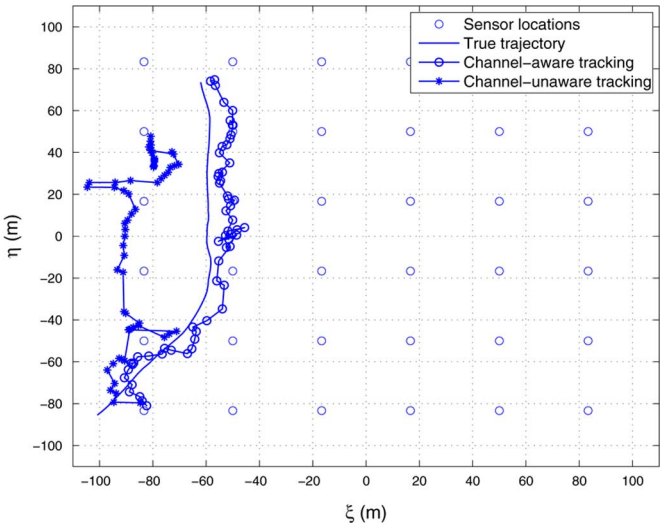

Fig. 3. Example of the tracking framework. (BER $p = 0.05, \rho = 9 \times 10^{-4}$ $\mathrm{m}^{-2}, \gamma_1 = 1.7$.)

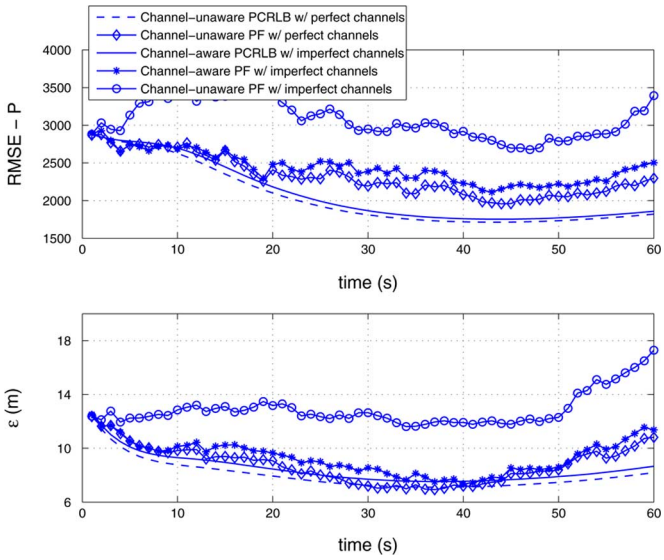

Fig. 4. RMSEs of channel-aware and channel-unaware PFs using binary data compared to their theoretical PCRLB in meters. (BER $p = 0.01$ for imperfect channel cases, $\rho = 9 \times 10^{-4}$ $\mathrm{m}^{-2}, \gamma_1 = 1.7$.)

mean $\boldsymbol{\mu}_{x_0} = [25000 \quad -80 \quad -80 \quad 2 \quad 2]^T$ and covariance $\boldsymbol{\Sigma}_{x_0} = \mathrm{diag}[3000^2 \quad 10^2 \quad 10^2 \quad .5^2 \quad .5^2]$. The standard deviation of the process noise for the target signal power dynamic model is $\sigma_\beta = 500$. The target motion follows a near constant velocity model with a process noise parameter, $q = 0.04$. Measurements are assumed to be taken at regular intervals of 1 s, i.e., $T_s = 1$, and the observation length is 60 s. The number of particles used for all the particle filters is 1000.

First, in Section VI-A, we assess the tracking performance of our channel-aware particle filtering algorithm assuming hard-decoding links and imperfect channel conditions, namely BCs, and perform a comparison with the existing channel-unaware particle filtering algorithm. For simplicity, we further assume that probability of making a wrong decision for each bit is identical, i.e., bit-error-rate $(\mathrm{BER}) = p = q$, forming a BSC model. Second, in Section VI-B, we evaluate the tracking performance of our channel-aware particle filters assuming soft-decoding links (coherent and noncoherent) and demonstrate the performance gains by employing the soft-decoding receiver architecture. Note that without obtaining channel state information (CSI), it is impossible to employ channel-unaware tracking algorithms using a soft-decoding scheme, which is another advantage gained by incorporating channel statistics directly in the tracking algorithm. Finally, in Section VI-C, we investigate the effects of link-layer designs on tracking performance.

A. Binary Symmetric Channel

Based on the fact that $p = q$ for a BSC, we will omit the symbol q and use symbol p alone to indicate the bit-error probability throughout this subsection. In order to visually assess the performance improvement by employing channel-aware processing for tracking, we give an example track in Fig. 3, where we compare our channel-aware particle filtering approach with its channel-unaware counterpart. Both filters use binary data received from 36 sensors ($\rho = 9 \times 10^{-4}$ m^{-2}), which are grid-deployed in the region as shown in Fig. 3. The channels are modeled as BSCs with BERs equal to 0.05. Since binary data is used, there is only one threshold, γ_1, and it is set to 1.7 for the 1-bit quantization [7]. As can be seen from the figure, the channel-aware PF is able to keep the track very close to the true target trajectory whereas the channel-unaware PF loses the track.

Fig. 4 is a more clear demonstration of both the motivation behind our channel-aware particle filtering approach and the significant performance gain achieved by this approach. First, we demonstrate two different scenarios in which we investigate the performance of the channel-unaware PF. In the first scenario, all the channels are modeled as perfect whereas in the second scenario the channels are modeled as BSCs with BERs equal to 0.01. In Fig. 4, the performance of the channel-unaware PF estimator using binary data for these two different scenarios is shown as a function of time. PCRLB for the channel-unaware PF (channel-unaware PCRLB) is also provided as a performance measure. Note that the main performance criterion is the root mean square error (RMSE) of the target position estimates defined by $\varepsilon_k \triangleq \sqrt{(\xi_{tk} - \hat{\xi}_{tk})^2 + (\eta_{tk} - \hat{\eta}_{tk})^2}$. Although target signal power P_k is a nuisance parameter, the RMSEs of P_k estimates are also shown in Fig. 4. PCRLB and RMSE values are computed based on 100 Monte Carlo trials. As is clearly seen in Fig. 4, the channel-unaware PF has significant performance degradation for the scenario when channels are not perfect. As a second demonstration in Fig. 4, the performance of the channel-aware PF using binary data is compared with its theoretical PCRLB as a function of time. All the parameters are kept the same as those used in the channel unaware scenarios. It is clearly seen that the performance degradation due to imperfect channels becomes almost negligible when the channel-aware PF is employed. It is also obvious that the performance of channel-aware PF is also quite close its PCRLB and it significantly outperforms the channel-unaware PF when channels are imperfect. Furthermore, the channel-aware PCRLB provides a much tighter performance bound for the target tracking problem with imperfect channels.

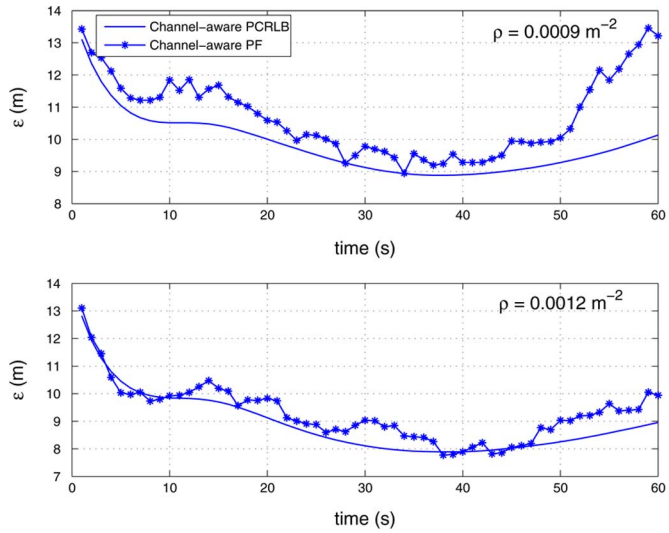

Fig. 5. RMSEs of channel-aware PFs using binary data compared to their PCRLBs for different sensor densities $(\rho) \cdot (p = 0.0642, \gamma_1 = 1.7)$.

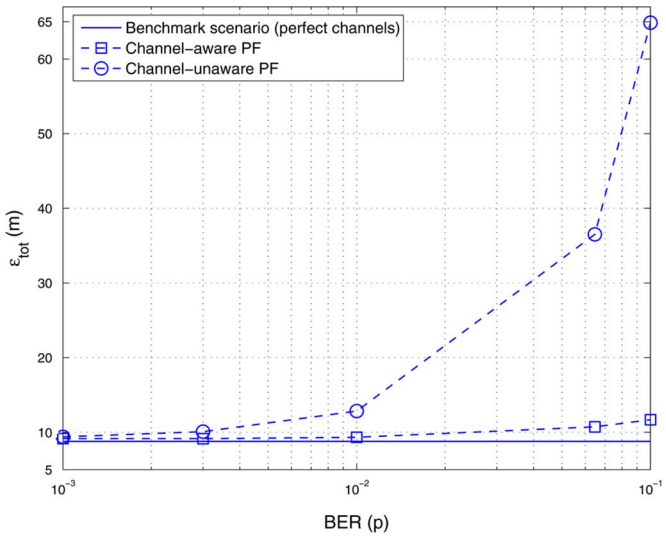

Fig. 6. RMSEs of channel-aware and channel-unaware PFs using binary data with respect to different bit error probabilities. ($\rho = 9 \times 10^{-4}$ m$^{-2}, \gamma_1 = 1.7, K = 60$.)

TABLE I
NUMBER OF LOST TRACKS IN 100 MONTE CARLO TRIALS

	$p = 0.01$	$p = 0.0642$
Channel-aware PF ($\rho = 9 \times 10^{-4}$)	0	1
Channel-unaware PF ($\rho = 9 \times 10^{-4}$)	3	30
Channel-aware PF ($\rho = 1.2 \times 10^{-3}$)	0	0
Channel-unaware PF ($\rho = 1.2 \times 10^{-3}$)	4	43

In Fig. 5, we consider a more realistic scenario, where each channel between the sensors and the fusion center is modeled as a coherent hard-decoding Rayleigh fading link with an average channel signal-to-noise ratio (SNR) of 5 dB. It is shown in [24] that for antipodal signaling (BPSK), where $m_i = \pm A$, a hard-decoding link forms a binary symmetric channel (BSC) and the error probability P_e for the corresponding fading channel is given by

$$P_e = \frac{1}{2}\left(1 - \sqrt{\frac{\mathrm{SNR}}{1+\mathrm{SNR}}}\right) \tag{53}$$

where $\mathrm{SNR} = \frac{A^2}{N_0}\overline{h^2}$ and $N_0/2$ is the power spectral density (PSD) of the additive noise. The expression in (53) can be used to calculate the BER as a function of SNR for each link from sensor i to the fusion center, where $i = 1, \ldots, N$. For our scenario where $\mathrm{SNR} = 5$ dB and $\overline{h^2} = 1$, the corresponding BER $p = 0.0642$. Fig. 5 shows the corresponding RMSE and PCRLB values based on 100 Monte Carlo trials for different sensor densities. It is clearly seen from Fig. 5 that as the sensor density increases, the performance of the channel-aware PF improves and converges to its PCRLB for almost all time instants. Even when the sensor density is relatively small, the performance of the channel-aware PF is quite close to its PCRLB.

Next, we define a lost track when the estimation error of the target position estimate is both greater than 10 m and is increasing in ten consecutive time steps. Based on this definition, Table I shows the number of lost tracks corresponding to channel-aware and channel-unaware particle filters for 100 Monte Carlo trials for BERs $p = 0.01$ and $p = 0.0642$. It is clear from Table I that the channel-unaware PF results in significant number of lost tracks when the channel gets worse whereas the channel-aware PF is very robust to channel imperfections. It is also interesting to note that the performance of the channel-unaware PF gets poorer when the sensor density increases. It is due to the fact that when the number of sensors increases, the received observation vector at the fusion center at each time step contains more errors for a given BER.

Finally, the performances of channel-aware and channel-unaware PFs are compared with respect to different bit error probabilities, p in Fig. 6. Both filters use binary data to track the target and the sensor density ρ is set to 9×10^{-4} m^{-2}. The performance criterion in this case is the total RMSE of the target position estimates, $\varepsilon_{\mathrm{tot}}$ given by

$$\varepsilon_{\mathrm{tot}} = \frac{1}{K}\sum_{k=1}^{K} \varepsilon_k \tag{54}$$

where K is the predefined final time of the track. We also set up a benchmark case where all the channels are modeled as perfect. As can be seen in the figure, the performance of the channel-unaware PF degrades significantly as the channel gets worse, i.e., as p increases. However, the performance of the channel-aware PF is quite robust to imperfections of the wireless channels since channel statistics have been included in the estimation process. Furthermore, the comparison with respect to the benchmark case shows that by employing channel-aware processing, we can reduce the degradation in the tracking performance due to channel imperfections such that it is almost negligible for $p \leq 0.01$.

B. Rayleigh Fading Channel

In this subsection, we assess the performances of our channel-aware particle filters developed for Rayleigh fading soft-decoding links. Channels are modeled as unit power Rayleigh fading channels, i.e., $\overline{h^2} = 1$, and the average channel SNR is set to 5 dB. Fig. 7 shows the tracking performance of the channel-aware PFs for two different reception techniques

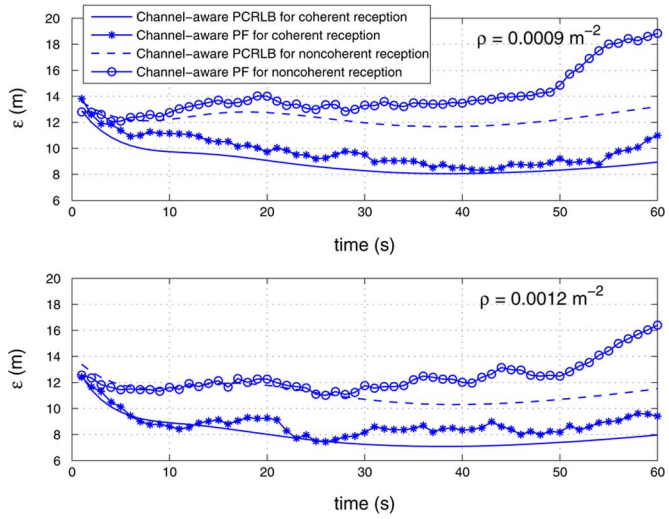

Fig. 7. RMSEs of channel-aware PFs for Rayleigh fading channel with coherent and noncoherent receptions compared to their PCRLB for different sensor densities (ρ). (Channel $\mathrm{SNR} = 5$ dB, $\gamma_1 = 1.7$.)

employed at the fusion center, namely phase coherent reception and phase noncoherent reception. Similar to the previous section, both RMSE and PCRLB values are computed based on 100 Monte Carlo trials. Antipodal signaling with unit amplitude ($m_i = \pm 1$) is adopted for the coherent reception scenario whereas the noncoherent reception scenario employs ON/OFF signaling ($m_i = 0$ or 1). Similar to our results for the BSC scenario, it is clear from Fig. 7 that the performances of the channel-aware particle filters for Rayleigh fading soft-decoding links are very close to their PCRLBs using relatively small number of sensors. Moreover, as it is already expected, for the same channel SNR and the same sensor density, the coherent receiver outperforms the noncoherent receiver in terms of target tracking since the former incorporates phase information of the received signal. However, the trade-off is the need for the exact knowledge of the phase of the channel resulting in extra energy consumption and the complexity of the receiver.

C. Comparison of Link Layer Designs

In this subsection, we evaluate the effects of different link layer designs on tracking performance under identical channel conditions. The goal of this evaluation is to give some insight to the designer about the role of the physical layer on tracking performance so that the designer can make decisions as to how to modify an existing tracking system or how to design a new tracking system using a WSN for a given performance requirement. The link layer designs we evaluate are 1) Rayleigh fading coherent soft-decoding link with channel-aware processing, 2) Rayleigh fading noncoherent soft-decoding link with channel-aware processing, 3) Rayleigh fading coherent hard-decoding link with channel-aware processing, 4) Rayleigh fading coherent hard-decoding link with channel-unaware processing, 5) Rayleigh fading noncoherent hard-decoding link with channel-aware processing, and 6) Rayleigh fading noncoherent hard-decoding link with channel-unaware processing. For all scenarios, binary signaling is employed and the sensor density is set to 1.2×10^{-3} m^{-2}. Note that as long as the channel statistics are known, any hard-decoding link can be modeled as a BC by deriving its corresponding bit error probabilities as a function of average channel SNR. Then, the particle filtering algorithm developed in Section IV-A can be used to evaluate the performance. Therefore, given a particular communication channel, in order to perform a comparison between hard-decoding links and soft-decoding links, the corresponding bit error probabilities need to be derived to be used in the particle filtering algorithm for the hard-decoding link, i.e., the corresponding BC link. Recall from Section VI-A that a coherent hard-decoding link with antipodal signaling forms a BSC with an error probability P_e given in (53), which can be used to calculate the BER as a function of SNR for Rayleigh fading coherent hard-decoding links. In addition, for a Rayleigh fading noncoherent hard-decoding link with ON/OFF signaling, we have derived the corresponding P_e which is stated in the following lemma.

Proposition 1: For ON/OFF signaling scheme, where either $m_i = 0$ or $m_i = B$ is transmitted, the error probability is given by

$$P_e = \frac{1}{2}[P(\text{decide } B|m_i = 0) + P(\text{decide } 0|m_i = B)] = \frac{1}{2}\left[1 - \frac{2\mathrm{SNR}}{(2\mathrm{SNR}+1)^{\frac{2\mathrm{SNR}+1}{2\mathrm{SNR}}}}\right] \quad (55)$$

where

$$P(\text{decide } B|m_i = 0) = \left(\frac{1}{2\mathrm{SNR}+1}\right)^{\frac{2\mathrm{SNR}+1}{2\mathrm{SNR}}} \quad (56)$$

$$P(\text{decide } 0|m_i = B) = 1 - \left(\frac{1}{2\mathrm{SNR}+1}\right)^{\frac{1}{2SNR}} \quad (57)$$

and $\mathrm{SNR} = \frac{B^2}{2N_0}\overline{h^2}$.

We skip the Proof of Proposition 1 in this paper for the sake of brevity. Note that noncoherent reception for a Rayleigh fading hard-decoding link results in a binary nonsymmetric channel model with error probabilities provided by (56) and (57).

The performances of particle filters for six different link layer designs are shown in Fig. 8. Each RMSE value is computed based on 100 Monte Carlo trials. It is clear from the figure that channel-unaware PFs are consistently outperformed by the channel-aware PFs no matter which reception scheme is used at the receiver. Note also that noncoherent hard-decoding link with channel-unaware approach requires a much higher SNR value to reach its asymptotic performance compared to other link layer designs. This result indicates that if the employed receiver is noncoherent, channel-aware processing is crucial for good performance even when the channel SNR is relatively high. Among channel-aware particle filters, the tracking performances of coherent receivers are better than those of the noncoherent receivers as expected. If a design choice has to be made between coherent and noncoherent receivers, the choice can be made to optimize the overall performance of the system depending on the channel conditions, available resources and tolerable RMS errors for a specific tracking application, based on the fact that coherent receivers are more expensive to build and operate. Furthermore, soft-decoding schemes always perform better than the

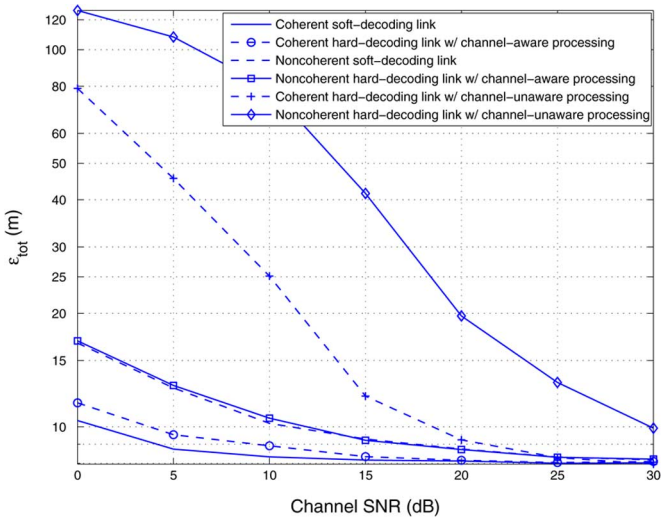

Fig. 8. RMSEs of channel-aware and channel-unaware PFs using binary data with respect to different average channel SNRs. ($\rho = 1.2 \times 10^{-3}$ m$^{-2}, \gamma_1 = 1.7$) for hard-decoding links.)

corresponding hard-decoding schemes, which would not be possible without a channel-aware approach. Incorporating channel-aware data processing directly in the tracking algorithm enables us to utilize soft-decoding link designs resulting in improved performance without adding any communication cost to the system.

VII. Summary and Discussion

In this paper, we studied the problem of target tracking using a resource constrained WSN with nonideal wireless channels. We have developed a new target tracking approach using Monte Carlo based statistical signal processing, which we refer to as channel-aware particle filtering. Our new approach uses quantized sensor data and incorporates wireless channel information as well as decoding scheme characteristics at the receiver. Three different types of channel-aware particle filters have been developed for three different link layer designs, namely hard-decoding links modeled as BCs, Rayleigh fading coherent soft-decoding links and Rayleigh fading noncoherent soft-decoding links. In addition, we have introduced a methodology to compute the PCRLB by using Monte Carlo methods for the developed channel-aware particle filters and showed that the tracking performance of the filters converges to their PCRLBs even with a relatively small number of sensors. We have also evaluated the effects of different link layer designs on tracking performance. This type of evaluation is useful at the design stage and can be utilized to design parameters and functions of the physical layer in order to optimize performance. Simulation results have shown that the performance of channel-aware particle filtering is strictly better than that of channel-unaware particle filtering. Furthermore, channel-aware data processing makes it possible to employ soft-decoding at the fusion center resulting in improved performance over corresponding hard-decoding links with no additional communication cost to the system. We have shown in this paper that the performance of a tracking application can be optimized by considering the WSN system as a whole so that a system-wide optimization can be performed. We have specifically demonstrated that the tracking algorithm at the fusion center and the physical layer of the network can be designed jointly for an improved overall system performance.

The optimal design of local sensor thresholds has not been studied in this paper. Thresholds can also be considered as design parameters for improved tracking performance. Note also that the performances of channel-aware particle filters are dependent on how accurate the channel models are. A robustness analysis needs to be carried out to see how the channel model mismatches affect the overall system performance. In addition, the channel aware framework that we have developed in this paper can be extended to include more complicated scenarios such as environments with multiple targets, clutters, out-of-sequence sensor measurements and dense sensor situations that require sensor selection approaches.

Appendix A
Proof of Theorem 1

As shown in (43), the outer expectations in the elements of $D_k^{22,b}$ can be approximated as summations using a set of particles. However, the inner expectation still remains to be evaluated. We first start with the (1,1) element of $D_k^{22,b}$

$$\Lambda_{1,1}^k \approx \frac{1}{M}\sum_{j=1}^{M} -E_{p(\mathbf{Y}_{k+1}|\mathbf{x}_{k+1}^{(j)})} \times \left\{ \frac{\partial^2 \log p\left(\mathbf{Y}_{k+1}|\mathbf{x}_{k+1}^{(j)}\right)}{\partial P_{k+1}^{(j)^2}} \right\}. \quad (58)$$

Omitting the time index k, and using (16), we have

$$\frac{\partial \ln p(\mathbf{Y}|\mathbf{x})}{\partial P} = \sum_{i=1}^{N} \frac{1}{p(\tilde{m}_i|\mathbf{x})} \frac{\partial p(\tilde{m}_i|\mathbf{x})}{\partial P} \quad (59)$$

$$\frac{\partial^2 \ln p(\mathbf{Y}|\mathbf{x})}{\partial P^2} = \sum_{i=1}^{N} -\frac{1}{p^2(\tilde{m}_i|\mathbf{x})}\left[\frac{\partial p(\tilde{m}_i|\mathbf{x})}{\partial P}\right]^2 + \frac{1}{p(\tilde{m}_i|\mathbf{x})}\frac{\partial^2 p(\tilde{m}_i|\mathbf{x})}{\partial P^2}. \quad (60)$$

Now, the expectation is calculated with respect to $p(\tilde{m}_i|\mathbf{x}))$:

$$\begin{aligned} &-E\left[\frac{\partial^2 \ln p(\mathbf{Y}|\mathbf{x})}{\partial P^2}\right] \\ &= \sum_{i=1}^{N}\sum_{\tilde{m}_i=0}^{L-1} -p(\tilde{m}_i|\mathbf{x})\left\{-\frac{1}{p^2(\tilde{m}_i|\mathbf{x})}\left[\frac{\partial p(\tilde{m}_i|\mathbf{x})}{\partial P}\right]^2 + \frac{1}{p(\tilde{m}_i|\mathbf{x})}\frac{\partial^2 p(\tilde{m}_i|\mathbf{x})}{\partial P^2}\right\} \\ &= \sum_{i=1}^{N}\sum_{\tilde{m}_i=0}^{L-1}\left\{\frac{1}{p(\tilde{m}_i|\mathbf{x}))}\left[\frac{\partial p(\tilde{m}_i|\mathbf{x}}{\partial P}\right]^2 - \frac{\partial^2 p(\tilde{m}_i|\mathbf{x})}{\partial P^2}\right\}. \end{aligned} \quad (61)$$

The second term in (61) is

$$\sum_{i=1}^{N}\sum_{\tilde{m}_i=0}^{L-1}\frac{\partial^2 p(\tilde{m}_i|\mathbf{x})}{\partial P^2} = \sum_{i=1}^{N}\frac{\partial^2}{\partial P^2}\left[\sum_{\tilde{m}_i=0}^{L-1} p(\tilde{m}_i|\mathbf{x})\right] = 0 \quad (62)$$

since $\sum_{\tilde{m}_i=0}^{L-1} p(\tilde{m}_i|\mathbf{x}) = 1$. Therefore, the expectation reduces to

$$-E\left[\frac{\partial^2 \ln p(\mathbf{Y}|\mathbf{x})}{\partial P^2}\right] = \sum_{i=1}^{N}\sum_{\tilde{m}_i=0}^{L-1} \frac{1}{p(\tilde{m}_i|\mathbf{x})}\left[\frac{\partial p(\tilde{m}_i|\mathbf{x})}{\partial P}\right]^2. \quad (63)$$

It is easy to see that the partial derivative term in (63) is

$$\frac{\partial p(\tilde{m}_i|\mathbf{x})}{\partial P} = \sum_{m_i=0}^{L-1} p(\tilde{m}_i|m_i)\frac{\partial p(m_i|\mathbf{x})}{\partial P}. \quad (64)$$

Then the following can be derived in a straightforward manner

$$\begin{aligned}\frac{\partial p(m_i = l|\mathbf{x})}{\partial P} &= \frac{\partial}{\partial P}\left[Q\left(\frac{\gamma_{il} - a_i}{\sigma_w}\right) - Q\left(\frac{\gamma_{i(l+1)} - a_i}{\sigma_w}\right)\right] \\ &= \frac{d_i^{-\frac{n}{2}}}{2\sqrt{2\pi}\sigma_w\sqrt{P}}\left[e^{\frac{-(\gamma_{il}-a_i)^2}{2\sigma_w^2}} - e^{\frac{-(\gamma_{i(l+1)}-a_i)^2}{2\sigma_w^2}}\right]. \quad (65)\end{aligned}$$

Following a similar procedure, it is easy to derive other elements of $D_k^{22,b}$. The derivation is skipped here for the sake of brevity.

Appendix B
Proof of Theorem 2

We first derive the (1,1) element of $D_k^{22,b}$. By using (24), we have the same expressions as in (59) and (60). Following a similar procedure as in Appendix A, we have

$$-E\left[\frac{\partial^2 \ln p(\mathbf{Y}|\mathbf{x})}{\partial P^2}\right] = \sum_{i=1}^{N}\int_{-\infty}^{\infty}\left(\frac{1}{p(\tilde{m}_i|\mathbf{x})} \times \left[\frac{\partial p(\tilde{m}_i|\mathbf{x})}{\partial P}\right]^2 - \frac{\partial^2 p(\tilde{m}_i|\mathbf{x})}{\partial P^2}\right) d\tilde{m}_i. \quad (66)$$

Note that (66) utilizes the fact that received observation $\tilde{m}_i$ is a real number and can take any value in $(-\infty, \infty)$ for the coherent soft-decoding scheme. Similar to the derivation in Appendix A, the second term in (66) vanishes. Therefore, the final expectation is of the form

$$-E\left[\frac{\partial^2 \ln p(\mathbf{Y}|\mathbf{x})}{\partial P^2}\right] = \sum_{i=1}^{N}\int_{-\infty}^{\infty}\frac{1}{p(\tilde{m}_i|\mathbf{x})}\left[\frac{\partial p(\tilde{m}_i|\mathbf{x})}{\partial P}\right]^2 d\tilde{m}_i \quad (67)$$

where the first term, $p(\tilde{m}_i|\mathbf{x})$ has been provided by (23) and the second term is given as

$$\frac{\partial p(\tilde{m}_i|\mathbf{x})}{\partial P} = \sum_{m_i\in\{-1,1\}} p(\tilde{m}_i|m_i)\frac{\partial p(m_i|\mathbf{x})}{\partial P}. \quad (68)$$

Note that $\partial p(m_i|\mathbf{x})/\partial P$ in (68) has been derived in Appendix A.

Other elements of $D_k^{22,b}$ can be derived easily following a similar procedure. The derivation is skipped here for the sake of brevity.

Appendix C
Proof of Theorem 3

We first derive the (1,1) element of $D_k^{22,b}$. Following the same procedures as in Appendices A–B, we have

$$-E\left[\frac{\partial^2 \ln p(\mathbf{Y}|\mathbf{x})}{\partial P^2}\right] = \sum_{i=1}^{N}\int_{0}^{\infty}\frac{1}{p(\tilde{m}_i|\mathbf{x})}\left[\frac{\partial p(\tilde{m}_i|\mathbf{x})}{\partial P}\right]^2 d\tilde{m}_i \quad (69)$$

where the fact that $\tilde{m}_i = |r_i|^2 \in [0, \infty)$ has been used. Similarly, the expressions for the terms in the integration are already derived in Section IV-C and Appendix A, and other terms of $D_k^{22,b}$ can be derived following the same procedure. The derivation is skipped here for the sake of brevity.

References

[1] L. Zuo, K. Mehrotra, P. K. Varshney, and C. Mohan, "Bandwidth-efficient target tracking in distributed sensor networks using particle filters," in *Proc. Conf. Information Fusion (Fusion 2006)*, Florence, Italy, Jul. 2006.

[2] X. Sheng and Y. Hu, "Sequential acoustic energy based source localization using particle filter in a distributed sensor network," in *Proc. Int. Conf. Acoustics, Speech, Signal Processing (ICASSP)*, Montreal, QC, Canada, May 2004.

[3] D. Guo and X. Wang, "Dynamic sensor collaboration via sequential Monte Carlo," *IEEE J. Sel. Areas Commun.*, vol. 22, no. 6, pp. 1037–1047, Aug. 2004.

[4] P. M. Djuric, M. Vemula, and M. F. Bugallo, "Target tracking by particle filtering in binary sensor networks," *IEEE Trans. Signal Process.*, vol. 56, no. 6, pp. 2229–2238, Jun. 2006.

[5] Y. Ruan, P. Willett, A. Marrs, F. Palmieri, and S. Marano, "Practical fusion of quantized measurements via particle filtering," *IEEE Trans. Aerosp. Electron. Syst.*, vol. 44, no. 1, pp. 15–29, Jan. 2008.

[6] L. Zuo, R. Niu, and P. K. Varshney, "A sensor selection approach for target tracking in sensor networks with quantized measurements," in *Proc. Int. Conf. Acoustics, Speech, and Signal Processing (ICASSP)*, Las Vegas, NV, Apr. 2008.

[7] R. Niu and P. K. Varshney, "Target location estimation in sensor networks with quantized data," *IEEE Trans. Signal Process.*, vol. 54, no. 12, pp. 4519–4528, Dec. 2006.

[8] N. Katenka, E. Levina, and G. Michailidis, "Robust target localization from binary decisions in wireless sensor networks," Dept. of Statistics Univ. of Michigan, Tech. Rep. 452, Mar. 2007.

[9] O. Ozdemir, R. Niu, and P. K. Varshney, "Channel aware target localization with quantized data in wireless sensor networks," *IEEE Trans. Signal Process.*, vol. 57, no. 3, pp. 1190–1202, Mar. 2009.

[10] B. Chen, R. Jiang, T. Kasetkasem, and P. K. Varshney, "Channel aware decision fusion in wireless sensor networks," *IEEE Trans. Signal Process.*, vol. 52, no. 12, pp. 3454–3458, Dec. 2004.

[11] B. Chen and P. Willett, "On the optimality of the likelihood-ratio test for local sensor decision rules in the presence of nonideal channels," *IEEE Trans. Inf. Theory*, vol. 51, no. 2, pp. 693–699, Feb. 2005.

[12] R. Jiang and B. Chen, "Fusion of censored decisions in wireless sensor networks," *IEEE Trans. Wireless Commun.*, vol. 4, no. 6, pp. 2668–2673, Nov. 2005.

[13] R. Niu, B. Chen, and P. K. Varshney, "Fusion of decisions transmitted over Rayleigh fading channels in wireless sensor networks," *IEEE Trans. Signal Process.*, vol. 54, no. 3, pp. 1018–1027, Mar. 2006.

[14] B. Chen, L. Tong, and P. K. Varshney, "Channel-aware distributed detection in wireless sensor networks," *IEEE Signal Process. Mag. (Special Issue on Distributed Signal Processing for Sensor Networks)*, vol. 23, pp. 16–26, Jul. 2006.

[15] B. Liu and B. Chen, "Channel optimized quantizers for decentralized detection in wireless sensor networks," *IEEE Trans. Inf. Theory*, vol. 52, no. 7, pp. 3349–3358, Jul. 2006.

[16] Q. Cheng, B. Chen, and P. K. Varshney, "Detection performance limits for distributed sensor networks in the presence of nonideal channels," *IEEE Trans. Wireless Comm.*, vol. 5, no. 11, pp. 3034–3038, Nov. 2006.

[17] O. Ozdemir, R. Niu, and P. K. Varshney, "Channel aware particle filtering for tracking in sensor networks," in *Proc. Asilomar Conf. Signals, Systems, Computers*, Pacific Grove, CA, Oct. 2006.
[18] Y. Bar-Shalom, X. R. Li, and T. Kirubarajan, *Estimation with Applications to Tracking and Navigation*. New York: Wiley, 2001.
[19] Y. Hu and D. Li, "Energy-based collaborative source localization using acoustic micro-sensor array," *EURASIP J. Appl. Signal Process.*, vol. 2003, no. 1, pp. 321–337, Jan. 2003.
[20] C. Meesookho and U. Mitra, "On energy-based acoustic source localization for sensor networks," *IEEE Trans. Signal Process.*, vol. 56, no. 1, pp. 365–377, Jan. 2008.
[21] M. S. Arulampalam, S. Maskell, N. Gordon, and T. Clapp, "A tutorial on particle filters for online nonlinear/non-Gaussian Bayesian tracking," *IEEE Trans. Signal Process.*, vol. 50, no. 2, pp. 174–188, Feb. 2002.
[22] , A. Doucet, N. de Freitas, and N. Gordon, Eds., *Sequential Monte Carlo Methods in Practice*. New York: Springer, 2001.
[23] P. Tichavský, C. H. Muravchik, and A. Nehorai, "Posterior Cramér-Rao bounds for discrete-time nonlinear filtering," *IEEE Trans. Signal Process.*, vol. 46, no. 2, pp. 1386–1395, May 1998.
[24] D. Tse and P. Viswanath, *Fundamentals of Wireless Communication*. Cambridge, U.K.: Cambridge Univ. Press, 2005.

Onur Ozdemir (S'06) was born in Ankara, Turkey, on March 4, 1980. He received the B.S. degree in electrical and electronics engineering from Bogazici University, Istanbul, Turkey, in 2003, and the M.S. degree in electrical engineering from Syracuse University, Syracuse, NY, in 2004. Since 2004, he has been working towards the Ph.D. degree in electrical engineering at Syracuse University.

He was an intern at Mitsubishi Electric Research Laboratories, Cambridge, MA, in 2007 and 2009. His research interests are in the areas of statistical signal processing, data fusion, and their applications to sensor networks and wireless communications.

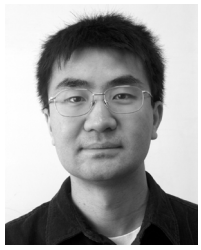

Ruixin Niu (M'04) received the B.S. degree from Xi'an Jiaotong University, Xi'an, China, in 1994, the M.S. degree from the Institute of Electronics, Chinese Academy of Sciences, Beijing, in 1997, and the Ph.D. degree from the University of Connecticut, Storrs, in 2001, all in electrical engineering.

He is currently a Research Assistant Professor with Syracuse University, Syracuse, NY. His research interests are in the areas of statistical signal processing and its applications, including detection, estimation, data fusion, communications and image processing.

Dr. Niu received the Fusion 2004 Best Paper Award, in the Seventh International Conference on Information Fusion, Stockholm, Sweden, in June 2004.

Pramod K. Varshney (F'97) was born in Allahabad, India, on July 1, 1952. He received the B.S. degree in electrical engineering and computer science (with highest honors) and the M.S. and Ph.D. degrees in electrical engineering from the University of Illinois at Urbana-Champaign in 1972, 1974, and 1976, respectively.

Since 1976, he has been with the Electrical and Computer Engineering Department, Syracuse University, Syracuse, NY, where he is currently a Distinguished Professor of electrical engineering and computer science. His current research interests are in distributed sensor networks and data fusion, detection and estimation theory, wireless communications, image processing, radar signal processing, and remote sensing. He has published extensively. He is the author of *Distributed Detection and Data Fusion* (New York: Springer-Verlag, 1997).

Dr. Varshney was a James Scholar, a Bronze Tablet Senior, and a Fellow while with the University of Illinois. He is a member of Tau Beta Pi and is the recipient of the 1981 ASEE Dow Outstanding Young Faculty Award. He was the Guest Editor of the Special Issue on Data Fusion of the *Proceedings of the IEEE*, January 1997. In 2000, he received the Third Millenium Medal from the IEEE and the Chancellor's Citation for Exceptional Academic Achievement at Syracuse University. He serves as a Distinguished Lecturer for the IEEE Aerospace and Electronic Systems (AES) Society. He is on the editorial boards of the *International Journal of Distributed Sensor Networks* and the IEEE TRANSACTIONS ON SIGNAL PROCESSING. He was the President of the International Society of Information Fusion during 2001.